Evanescent wave cavity ring-down spectroscopy: A new platform for thin-film chemical sensors

Andrew C. R. Pipino

Process Measurements Division
National Institute of Standards and Technology
100 Bureau Drive
Gaithersburg, Maryland 20899-8363

ABSTRACT

A new optical technique is described that permits extension of cavity ring-down spectroscopy (CRDS) to surfaces, films, and liquids. As in conventional CRDS, the photon intensity decay time in a low loss optical cavity is utilized to probe optical absorption. Extension to condensed matter is achieved by employing intra-cavity total internal reflection (TIR) to generate an evanescent wave that is especially well suited for thin film chemical sensing. Two general monolithic cavity designs are discussed: 1) a broadband, TIR-ring cavity that employs photon tunneling to excite and monitor cavity modes, and 2) a narrow bandwidth cavity that utilizes a combination of TIR and highly reflective coatings. Following a qualitative description of design features, a beam transfer matrix analysis is given which yields stability criteria and mode properties as a function of cavity length and mirror radius of curvature. A signal-to-noise ratio calculation is given to demonstrate the evaluation of sensitivity.

Keywords: Evanescent waves, optical absorption, cavity ring-down, resonator design, chemical sensing, films.

1. INTRODUCTION

Cavity ring-down spectroscopy[1-4] (CRDS) is a relatively new technique for the measurement of optical absorption that provides simplicity of operation with the (nearly realized) potential for achieving routine shot-noise-limited sensitivity at high fluence. CRDS utilizes the photon intensity decay time or "ring-down" time in a high-finesse optical cavity as the absorption-sensitive observable. Typically, the cavity is formed from a pair of narrowband, ultra-high reflectivity dielectric mirrors, configured to form a stable optical resonator. When light, usually from a pulsed or continuous wave laser, is injected into the cavity, the intensity decays exponentially with a ring-down time given by,

$$\tau(\omega)=\frac{t_r}{\mathcal{L}_0(\omega) + \mathcal{L}_{abs}(\omega)} \qquad (1)$$

where $\mathcal{L}_0(\omega)$ and $\mathcal{L}_{abs}(\omega)$ are the intrinsic and absorption loss, respectively, and t_r is the round-trip time for light propagation in the cavity. By measuring the difference in the intensity decay rate with and without an absorbing medium in the cavity as a function of laser frequency, the absolute absorption spectrum is obtained. Optical absorption is thereby transformed from a measurement of optical power to a measurement of time. The minimum detectable absorption in CRDS can be expressed[5] as the product of the intrinsic loss and the relative uncertainty in the ring-down time, or $(\mathcal{L}_{abs})_{min}=\mathcal{L}_0*(\Delta\tau/\tau)_{min}$, which separates approximately into cavity- and instrumentation-dependent terms, respectively. Therefore, sensitivity in CRDS can be optimized by minimizing the intrinsic cavity loss and measuring the ring-down time with the minimum uncertainty. Until recently, CRDS had been employed for gas phase diagnostics only since a large intrinsic cavity loss is introduced by most condensed matter sampling schemes such as liquid cells or film-coated plates. To minimize $\mathcal{L}_0(\omega)$, Fresnel reflections losses must be minimized or eliminated, along with other extraneous losses such as surface roughness scattering, residual absorption by optical materials or coatings, and diffraction losses arising from intra-cavity apertures. To realize a condensed matter implementation of CRDS, new cavity designs are

Part of the SPIE Conference on Advanced Materials and Optical Systems for Chemical and Biological Detection • Boston, Massachusetts • September 1999
SPIE Vol. 3858 • 0277-786X/99/$10.00

required that maintain a low intrinsic loss and provide simplicity of operation. Furthermore, a broad spectral bandwidth is also desirable since condensed matter spectra are typically broad. The ability to probe multiple spectral features or regions with a single cavity would also clearly be beneficial. Since the high reflectivity coatings that are typically employed in CRDS inherently possess a narrow spectral bandwidth, an alternative reflector is therefore required.

2. OPTICAL RESONATOR DESIGNS

By employing intracavity total internal reflection (TIR), both broad bandwidth and extremely low intrinsic loss can be achieved. Condensed matter sampling is accomplished with the associated evanescent wave, providing essentially a comprehensive extension of CRDS to condensed matter. This strategy, known as evanescent wave cavity ring-down spectroscopy (EW-CRDS), may ultimately permit routine single molecule detection. Several cavity designs that employ intracavity TIR have been explored.[6-10] In the first demonstration of EW-CRDS, the optical cavity was formed by a Pellin-Broca prism and a pair of conventional CRDS mirrors.[7] Sub-monolayer coverage of adsorbed iodine was detected by the change in ring-down time arising from evanescent wave absorption at the TIR surface of the prism. However, since the Pellin-Broca prism provided low loss only for p-polarization, a large contribution to $\mathfrak{L}_0(\omega)$ arising from depolarization by residual birefringence was introduced. The inability to vary polarization also precluded the measurement of molecular orientation and other polarization-dependent phenomena. In addition, since conventional CRDS mirrors were used, the cavity possessed a narrow spectral bandwidth. Since this early work, two new cavity designs have been realized experimentally: a broadband, monolithic TIR-ring cavity[6,8,9] and a monolithic, narrowband folded cavity.[10] Both resonators are described below and a general theoretical analysis is provided to facilitate the design of experiments. A signal-to-noise ratio calculation is then given to demonstrate the evaluation of minimum detectable absorption.

2.1 Total-internal-reflection-ring resonator

Depicted in Figure 1 in a nominally square geometry, the TIR-ring cavity has a broad bandwidth and a small, essentially polarization-independent intrinsic loss. For a ring cavity with N facets, the angle of incidence is given by $\theta_i=\pi(N-2)/2N$ and must exceed the critical angle $\theta_c=\sin^{-1}(n_2/n_1)$, where n_1 and n_2 are the refractive indices for the cavity and ambient medium, respectively. Since the cavity modes are sustained entirely by TIR, a broad bandwidth, which is

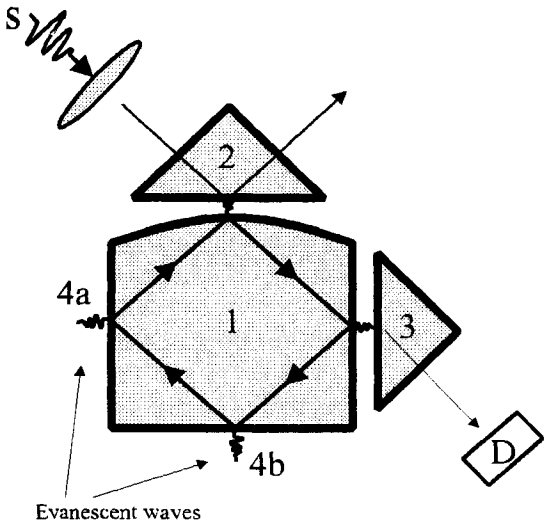

Figure 1. A miniature (<1 cm^3) polygonal, monolithic TIR-ring cavity (1) forms the basis for a novel, cavity ring-down miniature spectrometer for surfaces, films, and liquids. Elements 2 and 3 are used to couple light into and out of the solid cavity by photon tunneling, which is also known as frustrated-total-reflection (FTR). Evanescent waves at positions 4a-b probe the surrounding medium. Measurement of the decay rate of an injected light pulse permits accurate and absolute determination of absorption over the well-defined path length established by the evanescent wave decay length. Input and output light beams can be transported by fiber-optics to remotely locate the light source (S) and detector (D).

limited only by the transmission properties of the cavity medium, is obtained for a judicious choice of N that maintains $\theta_i > \theta_c$ throughout the high transmission region of the medium. A convex facet is required to form a stable resonator which supports low-diffraction-loss, self-replicating optical modes. Excitation and monitoring of cavity modes is accomplished by employing photon tunneling (also called 'frustrated total reflection'), which results in a gap-width dependent finesse.[11] Input coupling occurs at the convex facet, while a flat facet is used for output coupling. To align to

the system and optimize coupling, the cavity and coupling optics are mounted on a miniature optical breadboard that allows for control of all degrees of freedom relative to the incident laser source. On the miniature breadboard, micro-positioners provide control of all degrees of freedom for the coupling optics relative to the rigidly mounted cavity. Piezoelectric translators are required only for control of the tunneling junctions, which are probed interferometrically. A micro-optics implementation of the concept will allow a portable, fiber-optic-coupled, miniature spectrometer to be achieved.

The ring-down time for the TIR-ring cavity is given by Eq. 1, with the intrinsic loss given by,

$$\mathcal{L}_0(\omega)=\mathcal{L}_{bulk}+\mathcal{L}_{surf}+\mathcal{L}_{diff}+\mathcal{L}_{coup}+\mathcal{L}_{nspec} \quad \textbf{(2)}$$

where the loss terms correspond to bulk absorption and scattering, TIR surface scattering, diffractive attenuation by the finite cavity facets, coupling, and nonspecular losses, respectively. The magnitude and frequency dependence of each term in Eq. 2 have been examined in detail previously.[6] Since the bulk and diffraction losses have an opposing dependence on cavity size, an optimum size results at a given radius of curvature for the convex facet from the competition between these loss sources. Nonspecular losses can be neglected if θ_i-θ_c>1^0, while surface scattering losses can be minimized by "superpolishing" the cavity facets to 0.05 nm RMS surface roughness. The coupling loss, which is controlled by adjusting the tunneling junctions, is required to permit optical radiation to enter and exit the resonator. Under impedance-matched conditions where the coupling loss equals the round-trip loss, the cavity finesse reaches half the maximum value and the resonator transmission is near unity. At larger tunneling junctions, the finesse approaches a constant and maximum value, although the on-resonance transmission is reduced from unity. By employing high power laser sources and sensitive detection, operation in the weak coupling regime yields sufficient throughput, while providing stabilization and maximization of cavity finesse. The coupling loss is then small relative to the sum of other losses. With proper material selection, cavity design, and weak coupling, $\mathcal{L}_0(\omega)$ can be in the range of $1\text{x}10^{-7} \leq \mathcal{L}_0 \leq 1\text{x}10^{-3}$ over broad spectral regions, which yields long ring-down times that can be measured with high precision. Furthermore, because the TIR condition is satisfied for both in-plane (p-) and out-of-plane (s-) polarization states, polarization-dependent phenomena such as molecular orientation can be studied.

Surfaces, films, or liquids can be probed with the TIR-ring cavity by selecting an appropriate resonator geometry in accord with the TIR condition. General application to surfaces is achieved by probing a film that is thin relative to the evanescent wave decay length but sufficiently thick to achieve the chemical equivalence of a semi-infinite surface, since the TIR condition is not affected by the presence of such a film. Even when a strongly absorbing medium is of interest, a sparse distribution of islands, clusters, or adatoms, can be probed to investigate fundamental chemical interactions. Liquids can be probed by increasing the angle of incidence through an increase in the number of cavity facets, N, or through an increase in the refractive index of the cavity medium, n_1. For chemical sensing applications, the analyte of interest can be detected by direct adsorption on the TIR surface or selectivity can be enhanced by applying a selective film to the resonator surface.

2.2 Folded monolithic resonator

Since photon tunneling is used to excite the modes of the TIR-ring cavity, precise positioning and mounting of one or more coupling prisms is required to form a functional device. By employing an alternative monolithic, folded resonator design that employs both ultra-high reflective coatings and TIR, this complication is eliminated, though at the expense of a greatly reduced bandwidth. However, if the spectroscopy of a particular system is well-established, then for quantitative chemical sensing applications, a single wavelength can be monitored, eliminating the need for a broad bandwidth. For such applications, a folded monolithic resonator has several advantages including direct excitation by a propagating wave, high finesse for both polarization states, excellent stability, and simplicity of operation.

Depicted in Figure 2, the folded three-mirror resonator is formed from a monolithic solid of highly transmissive optical material with two ultra-high reflectivity coated surfaces and one convex TIR surface. A laser pulse is injected through a coated surface to excite a cavity mode. Following excitation, the exponentially decaying cavity output is detected at the second coated surface. The ring-down time for the folded cavity is also given by Eq. 1 but with the intrinsic loss given by,

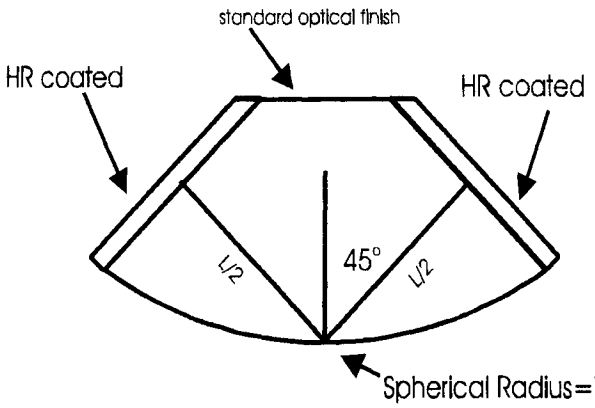

Figure 2. A monolithic, folded resonator for EW-CRDS is shown. The two high-reflectivity, coated surfaces and the convex TIR surface form a stable optical cavity. Light from a laser source is injected into the cavity through one of the coated surfaces to excite a cavity mode. The exponentially decaying intensity of the mode is detected as weak transmission through the second coated surface, enabling measurement of the ring-down time. The flat surface that is opposite the convex surface facilitates mounting and permits interferometry to be used for probing the thickness of films deposited on the convex TIR surface. The evanescent wave that emanates from the TIR surface probes the sample absorption.

$$\mathcal{L}_0(\omega)=\mathcal{L}_{bulk}+\mathcal{L}_C+\mathcal{L}_{surf}+\mathcal{L}_{diff}+\mathcal{L}_{nspec} \qquad (3)$$

where $\mathcal{L}_C=2(1-R(\omega))$ accounts for the reflection loss arising from the coated surfaces with reflectivity $R(\omega)$. Both coated and TIR surfaces are superpolished, reducing $\mathcal{L}_{surf}\sim10^{-6}$. L_{diff} is minimized by designing the resonator so that no effective intra-cavity apertures exist which attenuate the circulating intensity to a significant degree. Just as for the TIR-ring cavity, nonspecular losses can be rendered negligible by designing $\theta_i-\theta_c>1^0$. The absorption of an ambient medium is probed by the evanescent wave which emanates from the convex TIR surface. The polarization independence of TIR and the reflectivity of the coated surfaces at normal incidence assures that the folded cavity operates with high finesse for both in-plane and out-of-plane polarization states. A wide variety of polarization dependent phenomena can therefore be probed. Surfaces, films, and liquids can be studied using the folded cavity by varying the design angle of incidence to maintain the TIR condition. In Figure 2, $\theta_i=45°$ which is appropriate for diagnostics of surfaces and films in the visible and near-IR using a fused silica resonator and has been realized experimentally.[10] The folded resonator interfaces readily to experiments by mating the convex surface to a chamber or other apparatus by an O-ring seal. The single element design also stabilizes the resonance frequency since the alignment and cavity length are less susceptible to environmental variations. Single mode excitation is then facilitated, which improves decay time precision.[12]

3. THEORETICAL ANALYSIS

To provide guidance for the design of monolithic resonators for particular applications, a transfer matrix analysis of the stability criteria and beam properties is derived below as a function of basic resonator parameters. The stability criteria determine acceptable choices for the ratio of the radius of curvature to the round-trip path length of the resonator. When combined with a target ring-down time and minimum detectable absorption, the stability criteria yield the possible range for the radius of curvature of the convex facet. The waist size, location, and astigmatism are also determined from the round-trip transfer matrix to identify conditions for lowest-order mode matching. Since single mode excitation provides a significant improvement in decay time measurement precision, mode matching will likely be very important for future applications.

3.1 Monolithic TIR-ring resonator

As discussed in detail by Seigman,[13] a theoretical analysis of any resonator begins with the determination of the round-trip transfer matrix which is obtained as the product of the elemental matrices associated with translations, refractions, and reflections. From the transfer matrix, all of the basic mode properties can be obtained as a function of the matrix elements. For an N-sided regular, polygonal resonator having a single convex facet with radius of curvature R, the round-trip transfer matrix was found to be given by,

$$\begin{bmatrix} A & B \\ C & D \end{bmatrix} = \begin{bmatrix} 1 & \dfrac{Nd_0\sin(\pi/N)}{n_1} \\ \dfrac{-2n_1}{R_{eff}} & 1-\dfrac{2Nd_0\sin(\pi/N)}{R_{eff}} \end{bmatrix} \tag{4}$$

where d_0 is the inscribed circle diameter of the resonator and R_{eff} is the effective radius of curvature which is a function of R as described below. Note that the matrix is unimodular (i.e., AD-BC=1) as required.[14] From the trace of the transfer matrix the stability condition can be obtained according to $-1 \le (A+D)/2 \le 1$, which yields from Eq. 4,

$$-1 \le 1-\frac{Nd_0\sin(\pi/N)}{R_{eff}} \le 1 \tag{5}$$

where $L_{rt}=Nd_0\sin(\pi/N)$ is the round-trip path length through the resonator. If Eq. 5 is satisfied, then self-replicating, low-diffraction-loss modes exist which are well-described by the Hermite-Gauss or Laguerre-Gauss functions. Since the resonator modes are incident on the convex facet at an oblique angle of incidence, the TIR-ring resonator is inherently astigmatic with the effective radii of curvature in the tangential and sagittal planes given by,

$$R_T=R\cos\theta_i \tag{6}$$

and

$$R_S=\frac{R}{\cos\theta_i}, \tag{7}$$

respectively, which yields separate stability conditions for the two planes. Since the bulk attenuation is a linear function of L_{rt}, a target value for $\mathfrak{L}_{bulk}$ must first be selected that is based on the desired minimum detectable absorption and an experimentally accessible value of the ring-down time. Once these choices have been made, the range of R is established by Eq. 5, together with Eqs. 6 and 7.

Since the beam size at the TIR surface determines the sampled area, knowledge of the beam waist size and location can be useful. In general, the waist of the lowest order mode is obtained from,

$$\omega_0^2=\frac{-\lambda\left[1-\left(\dfrac{A+D}{2}\right)^2\right]^{1/2}}{\pi C} \tag{8}$$

where λ is the wavelength. For a monolithic ring resonator with a single convex facet, this yields

$$\omega_0^2=\frac{\lambda L_{rt}}{2\pi n_1}\left[\frac{2R_{eff}}{L_{rt}}-1\right]^{1/2}. \tag{9}$$

Employing Eqs. 6 and 7 together with the expression for L_{rt} to show the dependence on the number of facets, the tangential and sagittal waist dimensions are found to be given by,

$$\omega_{0x}^2 = \frac{\lambda_0 L_{rt}}{2\pi n_1}\left(\frac{2R\sin(\pi/N)}{L_{rt}}-1\right)^{1/2} \tag{10}$$

$$\omega_{0y}^2 = \frac{\lambda_0 L_{rt}}{2\pi n_1}\left(\frac{2R}{L_{rt}\sin(\pi/N)} - 1\right)^{1/2}, \tag{11}$$

respectively. The location of the waist is also determined from the round-trip transfer matrix according to

$$z = \frac{A-D}{2C} \tag{12}$$

which shows that the waist is always located opposite the convex facet at $L_{rt}/2$.

3.2 Monolithic Folded Resonator

For the monolithic folded resonator of Figure 2, the round trip transfer matrix was found to be given by,

$$\begin{bmatrix} 1-4\frac{L}{R_{eff}}+2\frac{L^2}{R_{eff}^2} & 2L-3\frac{L^2}{R_{eff}}+\frac{L^3}{R_{eff}^2} \\ -\frac{4}{R_{eff}}+4\frac{L}{R_{eff}^2} & 1-4\frac{L}{R_{eff}}+2\frac{L^2}{R_{eff}^2} \end{bmatrix} \tag{13}$$

where L is the unfolded length of the cavity and R_{eff} is the effective radius of curvature of the single convex facet. The conditions for stability are determined from the trace of Eq. 13, yielding

$$-1 \le 1-4\frac{L}{R_{eff}}+2\frac{L^2}{R_{eff}^2} \le 1. \tag{14}$$

Since the resonator is astigmatic, the effective radii of curvature in the tangential and sagittal planes are again given by Eqs. 6 and 7. This yields separate stability conditions which are given by,

$$0 \le \left(1-\frac{L\cos\Theta_i}{R}\right)^2 \le 1 \tag{15}$$

and

$$0 \le \left(1-\frac{L}{R\cos\Theta_i}\right)^2 \le 1 \tag{16}$$

for the tangential and sagittal planes, respectively.

By symmetry and Eq. 12, the monolithic folded cavity has two waists, each located at the planar, coated surfaces. From Eq. 8, a general expression for the waist radius can also be found, which is given by,

$$\omega_0^2 = \frac{\lambda}{\pi}(L/2)^{1/2}(R_{eff} - L/2)^{1/2}. \quad (17)$$

Using Eqs. 6 and 7, the tangential and sagittal waist radii were found to be,

$$\omega_{0x}^2 = \frac{\lambda}{\pi}(L/2)^{1/2}(R\cos\theta_i - L/2)^{1/2} \quad (18)$$

and

$$\omega_{0y}^2 = \frac{\lambda}{\pi}(L/2)^{1/2}(R/\cos\theta_i - L/2)^{1/2}. \quad (19)$$

Since the TIR surface, which is located at a distance L/2 from a cavity waist, is the sampling point, the dimensions of the sampled region can be important in applications. By propagating the astigmatic Gaussian mode according to standard equations, the lowest order mode beam radii at the TIR are found to be given by,

$$\omega^2{}_x(L/2) = \omega_{0x}^2\left[1 + \left(\frac{\lambda L}{2\pi\omega_{0x}^2}\right)^2\right] \quad (20)$$

and

$$\omega^2{}_y(L/2) = \omega_{0y}^2\left[1 + \left(\frac{\lambda L}{2\pi\omega_{0y}^2}\right)^2\right] \quad (21)$$

for the tangential and sagittal planes, respectively. The projected area of the sampling spot is then elliptical with an area of $\pi\omega_x(L/2)\omega_y(L/2)/\cos\theta_i$.

4. EVALUATION OF SENSITIVITY

To estimate the minimum detectable absorption for detection of a particular chromophore by EW-CRDS, the direction and magnitude of the evanescent wave electric field must be known. Knowledge of the electric field distribution is required since molecules or films can be oriented with respect to the field direction, thereby affecting the magnitude and polarization dependence of absorption.[15] Possessing both longitudinal and transverse character, the evanescent wave electric field components can be calculated from Maxwell's equations and the refractive indices of the cavity and ambient medium. Since the magnitude and direction of the field components differ for the in-plane (p) and out-of-plane (s) polarization states, measurement of the polarization dependence of absorption can probe molecular orientation or other polarization dependent phenomena. TIR also produces a moderate electric field enhancement that correspondingly enhances sensitivity.

To demonstrate the procedure for estimating the minimum detectable absorption of an EW-CRDS measurement, consider the detection of sub-monolayer coverage of a chromophore that adsorbs to the TIR surface of the resonator with its transition dipole oriented along the normal to the surface, which is taken to be the z-axis. The measurement of absolute coverage is a longstanding problem in surface science, requiring knowledge of both orientation and absorption cross section for the surface-bound species, which are typically not known. In general, the measured absorption loss is proportional to $\langle \boldsymbol{\mu}\cdot\mathbf{E}\rangle^2$, where $\boldsymbol{\mu}$ and $\mathbf{E}$ are the transition dipole moment and electric field,

respectively.[16] Since the absorption cross section is proportional to the absolute square of the transition moment and given $|E_z|^2=\Gamma_z|E_o|^2$, where Γ_z and E_o are the field enhancement and incident electric field, respectively, the round-trip absorption loss can be expressed as,

$$L_{abs} = \Gamma_z N_s \sigma_s(\omega)/\cos\theta_i = \Gamma_z \Theta N_o \sigma_s(\omega)/\cos\theta_i \quad \textbf{(22)}$$

for this particular case, where $\sigma_s(\omega)$ is the absorption cross section for the surface-bound molecule, and $\Theta=N_s/N_o$ is the coverage or ratio of the surface density of adsorbed molecules to the adsorption site density. The $\cos\theta_i$ term in the denominator of Eq. 22 accounts for the change in sampled area arising from oblique incidence at the TIR surface. The minimum detectable coverage for the oriented system described above can be estimated from $(\mathcal{L}_{abs})_{min}$ according to,

$$\Theta_{min} = \frac{\left(L_o \frac{\Delta\tau}{\tau}\right)\cos\theta_i}{N N_o \Gamma_z \sigma(\omega)}. \quad \textbf{(23)}$$

A generalization of Eq. 23 to account for an arbitrary orientation for the adsorbed chromophores can be easily obtained, though with slightly increased complexity. Consider as a specific example the detection of adsorbed water molecules (or surface hydroxyl groups) that are present at the nascent, superpolished surface of a fused-silica (SiO_2) resonator, since the SiO_2 surface has many technological applications and forms the support for many sensing films. Water has a moderately strong combination band at 1.38 μm with $\sigma_s(\omega)\approx\sigma_{gas}(\omega)\approx 10^{-18}$ cm^2/molecule. The bulk attenuation of selected low OH content fused silica around 1.38 μm is ~ 5 x 10^{-7} cm^{-1}, which yields $\mathcal{L}_0$~ 5 x 10^{-7} if a 1 cm round-trip pathlength and bulk-loss-limited conditions are assumed. To obtain the highest sensitivity, excitation of only the lowest order transverse cavity mode, TEM_{00}, must be employed to minimize the relative uncertainty $\Delta\tau/\tau$. Single transverse mode excitation is best accomplished with a narrow linewidth source, which also results in increased light throughput due to the improved match between source and cavity linewidth. By achieving shot noise limited detection at high fluence, the ultimate sensitivity will be achieved, which yields $\Delta\tau/\tau$~10^{-4}-10^{-5} with realistic parameters.[12] Assuming a square resonator as in Figure 1 is employed with Γ_z=7.14, N=4, and θ_i=45°, then Θ_{min} N_o=5x10^5 molecules/cm^2. Estimating the average spot size to be ~5x10^{-5} cm^2 for the four TIR surfaces of the resonator from Eqs.10 and 11, using R=2.3 cm, a limit of detection of ~25 molecules is estimated. Therefore, approaching the single molecule detection limit at room temperature appears feasible with the nascent resonator surface. If a chemically selective film is applied to the resonator surface, the effective intrinsic cavity loss will be increased in regions where the film absorbs. The analyte of interest should therefore absorb at a significantly different wavelength or shift the absorption spectrum of the film. However, for very thin films, based for example on Langmuir-Blodgett bilayers, the film absorption will be sufficiently small that operation of a sensor near wavelengths were the film absorbs should still be feasible.

ACKNOWLEDGMENTS

This work was supported by the Environmental Management Science Program of the Department of Energy under Contract DE-AI07-97ER62518.

REFERENCES

1. A. O'Keefe and D. A. G. Deacon, Rev. Sci. Instrum. **59**, 2544 (1988).
2. J. J. Scherer, J. B. Paul, A. O'Keefe, R. J. Saykally, *Chem. Rev.* **97**, 25, (1997).
3. M. D. Wheeler, S. M. Newman, A. J. Orr-Ewing, M. N. R. Ashfold, J. Chem. Soc. Faraday T. **94** (3), 337, (1998).
4. *Cavity-Ringdown Spectroscopy*, K. W. Busch and M. A. Busch, eds. (Oxford University Press, 1999).
5. P. Zalicki and R. N. Zare, J. Chem. Phys. **102**, 2708, (1995).
6. A. C. R. Pipino, J. W. Hudgens, R. E. Huie, Rev. Sci. Instrum. **68** (8), 2978, (1997).
7. A. C. R. Pipino, J. W. Hudgens, R. E. Huie, Chem. Phys. Lett. **280**, 104 (1997).
8. A. C. R. Pipino in Proceedings of SPIE, Vol. 3535, Boston, Mass. 1998.
9. A. C. R. Pipino, submitted.
10. A. C. R. Pipino, submitted.
11. S. Schiller, I. I. Yu, M. M. Fejer, and R. L. Byer, Opt. Lett. **17**, 378 (1992).
12. R. D. van Zee, J. T. Hodges, and J. P. Looney, Appl. Opt. **38**, 3951 (1999).
13. A. E. Seigman, *Lasers*, (University Science Books: Mills Valley, CA, 1986).
14. A. Gerrard and J. M. Burch, *Introduction to Matrix Methods in Optics*, (J. Wiley & Sons, London, 1975).
15. N. J. Harrick, *Internal Reflection Spectroscopy*, (Interscience Publishers, New York, 1967).
16. N. L. Thompson, Harden M. McConnell, Thomas P. Burghardt, *Biophys. J.* **46**, 739, (1984).

Disclaimer

Identification of specific commercial products in this paper is provided in order to specify procedures completely. In no case does such identification imply recommendation or endorsement by the National Institute of Standards and Technology, nor does it imply that such products have necessarily been identified as the best available for the purpose.